International Journal of Bioinformatics Research, ISSN: 0975–3087, Volume 2, Issue 1, 2010, pp-20-30

Structural and Functional analysis of glutathione peroxidase from *Ricinus communis* L. – a computational approach.

Sohini Gupta[1], Sabuj Saha[1], Paushali Roy[2], Protip Basu[2] and Sayak Ganguli[2]*
[1]Cell Biology, Molecular Biology, Genetics and Plant Biotechnology Laboratory, Post Graduate Department of Botany, Barasat Government College, Kolkata.
[*2]DBT-Centre for Bioinformatics, Presidency College, Kolkata, sayakbif@yahoo.com

Abstract- Oxidative stress in plants causes the induction of several enzymes, including superoxide dismutase (EC 1.15.1.1), ascorbate peroxidase (EC 1.11.1.11) and glutathione reductase (EC 1.6.4.2). The first two are responsible for converting superoxide to H_2O_2 and its subsequent reduction to H_2O, and the third is involved in recycling of ascorbate. Glutathione peroxidases (GPXs, EC 1.11.1.9) are a family of key enzymes involved in scavenging oxyradicals in animals. Only recently, indications for the existence of this enzyme in plants were reported. Genes with significant sequence homology to one member of the animal GPX family, namely phospholipid hydroperoxide glutathione peroxidase (PHGPX), were isolated from several plants. In this paper we report the homology modelling of the glutathione peroxidase protein from *Ricinus communis* L. and its interactions with its two substrates hydrogen peroxide and glutathione. Specific sites of interaction were identified and ligand binding pockets were also screened.
Keywords: *Ricinus communis* L. Delaunay triangulation, glutathione peroxidase, oxidative stress, accessible surface area, pocket identification

Introduction

Reactive oxygen species (ROS) are generated through an incomplete reduction of oxygen molecules during mitochondrial respiration and/or cytosolic metabolism. Exposure to exogenous stimuli such as radiation and redox cycling drugs might be an alternative pathway of ROS production. ROS perform physiological roles relevant to cell signaling and redox-status control [1,2], while unbalanced generation of these species induces detrimental oxidation of macromolecules including DNA, proteins, and lipids. To minimize ROS-derived damage, aerobic organisms have evolved a series of multi-layered enzymatic and non-enzymatic defense systems [3]. Distinct enzymatic activities such as catalase, glutathione peroxidase (GPx), and peroxiredoxin (PRx; also called thioredoxin peroxidase) have been well characterized from numerous taxa, as the major antioxidant defense mechanism. Selenium-containing GPx proteins reduce H_2O_2 and organic hydroperoxides by employing glutathione (GSH) as an electron donor. A total of eight GPx families have been described in mammals on the basis of primary structure, specific substrate accessibility, and spatial expression [4,5]. These homotetrameric isoenzymes conserve structural/ biochemical properties, however, a number of enzymes that have been classified into GPx4 (phospholipid hydroperoxide GPx; PHGPx) may function in monomeric forms and exhibit unique substrate availability. The enzymes can interfere directly with hydroperoxidized phospholipids in biomembranes. Proteins belonging to the other GPx families display substrate preference toward $H_2O_2$and protect against lipid peroxidation via a concerted operation with phospholipase [6]. PHGPx is the basis of a principal defense system that intimately participates in the repair of

disrupted biomembranes [7]. The vertebrate-specific GPx7 and GPx8 also lack the oligomerization loop, although their unique enzymatic properties are less understood [5]. Multiple isoenzymes showing primary structure similar to those of the mammalian PHGPxs have been described in plants, along with their respective subcellular expression profiles [8,9]. Plant enzymes possess a Cys residue instead of a selenocysteine (Sec) at the catalytic site, and prefer thioredoxin (Trx) as the electron source [9-11]. A pair of PHGPx-like proteins that effectively reduce the peroxides by adapting the Trx system has also been isolated from insect, yeast, and protozoa [12-15]. Interestingly, the green alga *Chlamydomonas reinhardtii* was likely to express both GHS-dependent (CrGPx1 and CrGPx2) and Trxdependent (CrGPx3–5) GPxs [16]. These observations have created a controversy regarding the classification of PHGPx-like proteins [8,9]. Conversely, a novel functional class of 'Trx GPx-like peroxidase (TGPx)' has been proposed to clarify the unique GPx group sharing a common evolutionary origin with the GSH-dependent GPxs [5]. The molecular basis for the differential preference has also been investigated and appeared to involve a 'resolving Cys' within the α2 helix of the Trx-dependent GPxs [5,18,19]. In this work we structurally analyze the *Ricinus communis* L., glutathione peroxidase, isolated under conditions of lead accumulation.

Material and Method:

Molecular modelling was performed using Modeller 9.2 and extensive homology search was performed at the PDB and other structural resources. Ramachandran Analysis was performed to determine the stability of the modeled structure and then the accessible surface areas were determined from the structure. Individual pockets of ligand interactions were obtained from the structure and were mapped with the ASA results. [20]

For identifying and measuring pockets, Delaunay triangulation, alpha shape, and discrete flow[21 – 25]. For the 2-D model, discrete flow is defined only for empty triangles, that is, those Delaunay triangles that are not part of the dual complex. An obtuse empty triangle "flows" to its neighboring triangle, whereas an acute empty triangle is a *sink* that collects flow from neighboring empty triangles.

Docking was done using Autodock – VINA and was rechecked using FLEX-X. Two specific ligands were used for the study – glutathione and hydrogen peroxide (H_2O_2).

Results and Discussion

The structure modeled was found to be stereochemically stable from the Ramachandran analysis (Fig 1) and each individual pocket residue was found to be associated with a high ASA value, which further provides evidence that the structure represents a viable model. The *Spiral Plot* is a new method to quickly notice the surface residues in a protein. These may be the residues of interest. These spiral plots are generated by sorting all residues by their relative solvent accessibility. The radius of the sphere representing each residue is proportional to the accessible surface area of that residue, thus enabling a visual estimate of more accessible residues. These residues are then arranged in form of a spiral, such that the inner residues in this spiral represent buried residues and more and more exposed residues come nearer to the outer ring of the spiral. (Fig 2). Hydrogen bonding abilities of all the residues were analyzed and fractional and residual asa's were calculated (Table 1& 2). Ligand binding sites and potential hydrophobic pockets were identified using the Delaunay triangulation and different pockets were identified and correlated with their high ASA values. (Fig 3). From the molecular docking studies it was found that the two favoured substrates of glutathione peroxidase– H_2O_2 and glutathione each show specificity of binding to the cysteine residues at position 111 and at position 130 respectively (Fig 4 and 5). Interestingly, each of these residues are part of two different pockets that were identified[26].

References

[1] Thannickal V.J., Fanburg B.L. (2000) *Am J Physiol Lung Cell Mol Physiol*, 279:L1005-L1028.

[2] Jackson M.J. (2005) *Philos Trans R Soc Lond B Biol Sci*, 360:2285-2291.

[3] Sies H. (1993) *Eur J Biochem*, 215:213-219.

[4] Arthur J.R. (2000) *Cell Mol Life Sci*, 57:1825-1835.

[5] Toppo S., Vanin S., Bosello V., Tosatto S.C.E. (2008) *Antioxid Redox Signal*, 10:1501-1513.

[6] Grossmann A., Wendel A. (1983) *Eur J Biochem*, 135:549-552.

[7] Imai H., Nakagawa Y. (2003*) Free Radic Biol Med*, 34:145-169.

[8] Rouhier N., Jacquot J.P. (2005) *Free Radic Biol Med.*,38:1413-1421.

[9] Navrot N., Collin V., Gualberto J., Gelhaye E., Hirasawa M., Rey P., Knaff D.B., Issakidis E., Jacpuot J.P., Rouhier N. (2006) *Plant Physiol*, 142:1364-1379.

[10] Herbette S., Lenne C., Leblanc N., Julien J.L., Drevet J.R., Roeckel-Drevet P. (2002) *Eur J Biochem*, 269:2414-2420.

[11] Jung B.G., Lee K.O., Lee S.S., Chi Y.H., Jang H.H., Kang S.S., Lee K., Lim D., Yoon S.C., Yun D.J., Inoue Y., Cho M.J., Lee S.Y. (2002) *J Biol Chem*, 277:12572-12578.

[12] Sztajer H., Gamain B., Aumann K.D., Slomianny C., Becker K., Brigelius-Flohé R., Flohé L. (2001) *J Biol Chem*, 276:7397-7403.

[13] Missirlis F., Rahlfs S., Dimopoulos N., Bauer H., Becker K., Hilliker A., Phillips J.P., Jäckle H. (2003) *Biol Chem*., 384:463-472.

[14] Tanaka T., Izawa S., Inoue Y. (2005) *J Biol Chem*., 280:42078-42087.

[15] Corona M., Robinson G.E. (2006) *Insect Mol Biol*., 15:687-701.

[16] Dayer R., Fischer B.B., Eggen R.I., Lemaire S.D. (2008) *Genetics*., 179:41-57.

[17] Holland D., Ben-Hayyim G., Faltin Z., Camoin L., Strosberg A.D., Eshdat Y. (1993) *Plant Mol Biol.,* 21:923-927.

[18] Maiorino M., Ursini F., Bosello V., Toppo S., Tosatto S.C.E., Mauri P., Becker K., Roveri A., Bulato C., Benazzi L., De Palma A., Flohé L. (2007) *J Mol Biol*., 365:1033-1046.

[19] Tosatto S.C.E., Bosello V., Fogolari F., Mauri P., Roveri A., Toppo S., Flohé L., Ursini F., Maiorino M. (2008) *Antioxid Redox Signal*., 10:1515-1526.

[20] Shandar Ahmad, M. Michael Gromiha, Hamed Fawareh and Akinori Sarai (2004) *BMC Bioinformatics*, 5:51

[21] Edelsbrunner H., Mucke E.P. (1994) *ACM Trans. Graphics*, 13:43-72.

[22] Edelsbrunner H. (1995) *Discrete Comput. Geom.*,13:415-440.

[23] Edelsbrunner H., Shah N.R. (1996) *Algorithmica*, 15:223-241.

[24] Facello M.A. (1995) *Computer Aided Geometric Design*., 12:349-370.

[25] Liang J., Edelsbrunner H., Woodward C. (1998) *Protein Science,* 7:1884-1897.

[26] Joe Dundas, Zheng Ouyang, Jeffery Tseng, Andrew Binkowski, Yaron Turpaz, and Jie Liang (2006) *Nucl. Acids Res*., 34:W116-W118.

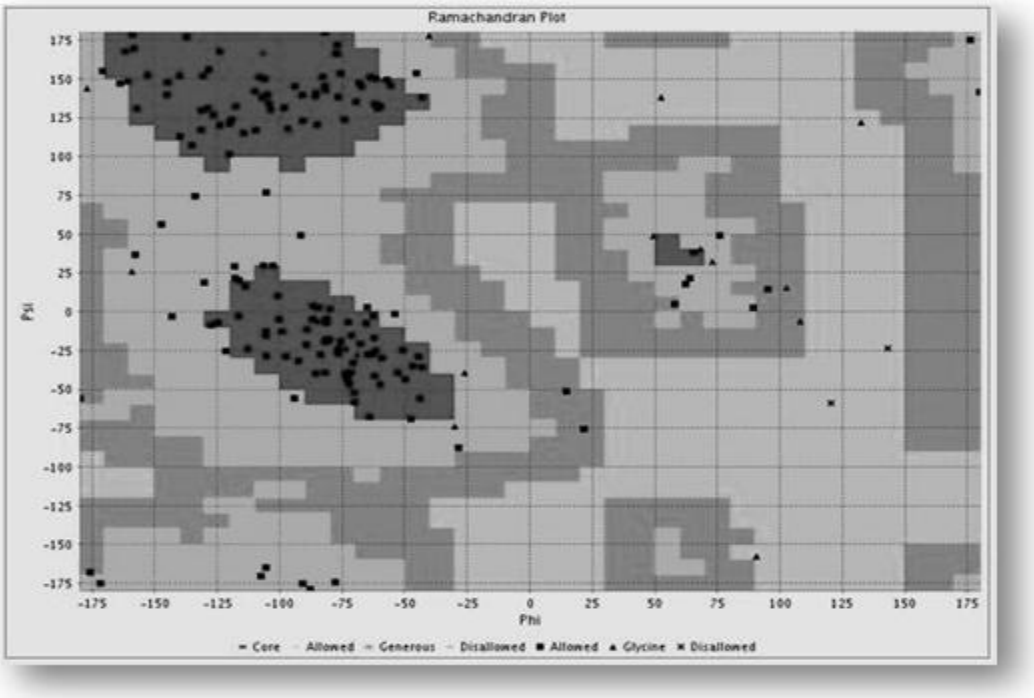

Fig. 1- Accessible surface area plot of glutathione peroxidase

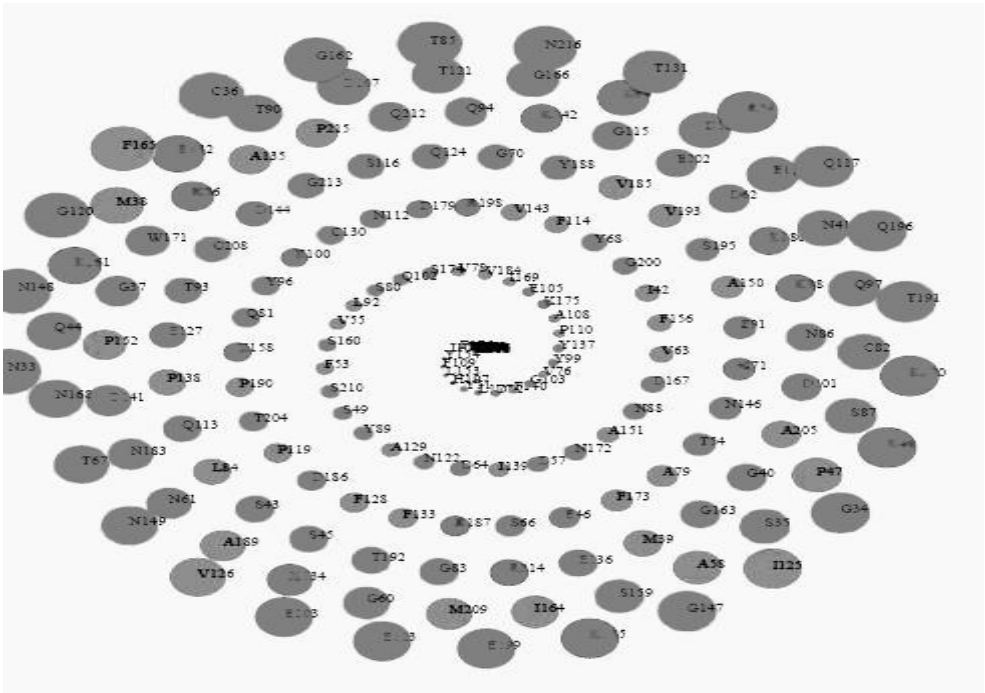

Fig. 2- Ligand binding pockets in the structure and their respective sequences (highlighted)

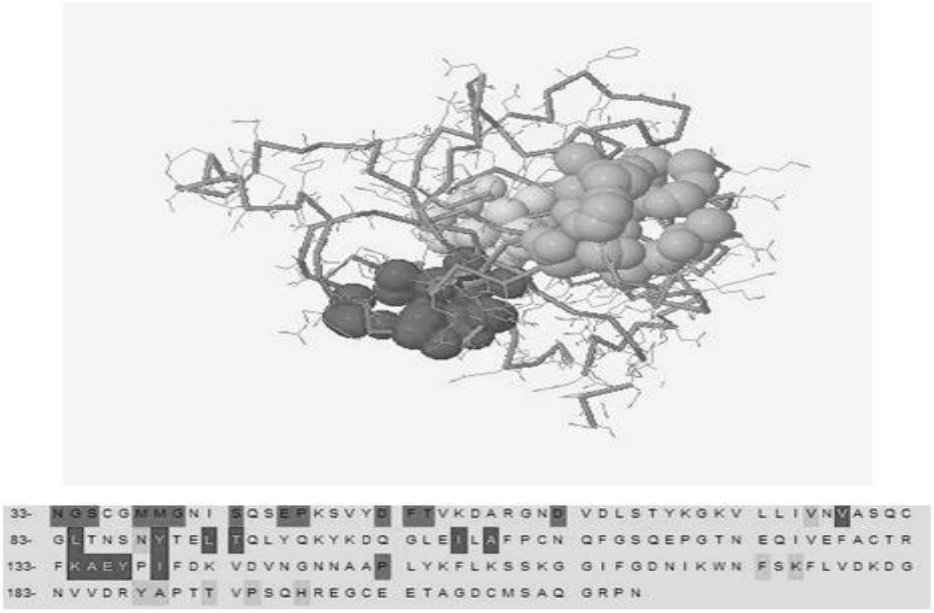

Fig. 3- Binding Interaction of Glutathione with the 3D structure of the enzyme

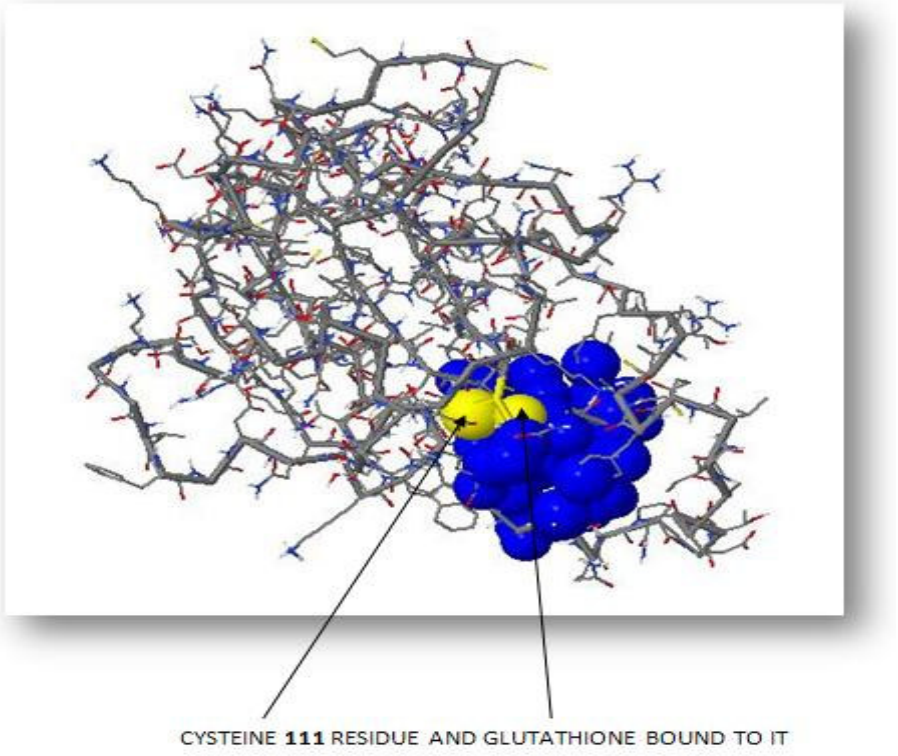

Fig. 4- Binding Interaction of Hydrogen Peroxide with the 3D structure of the enzyme

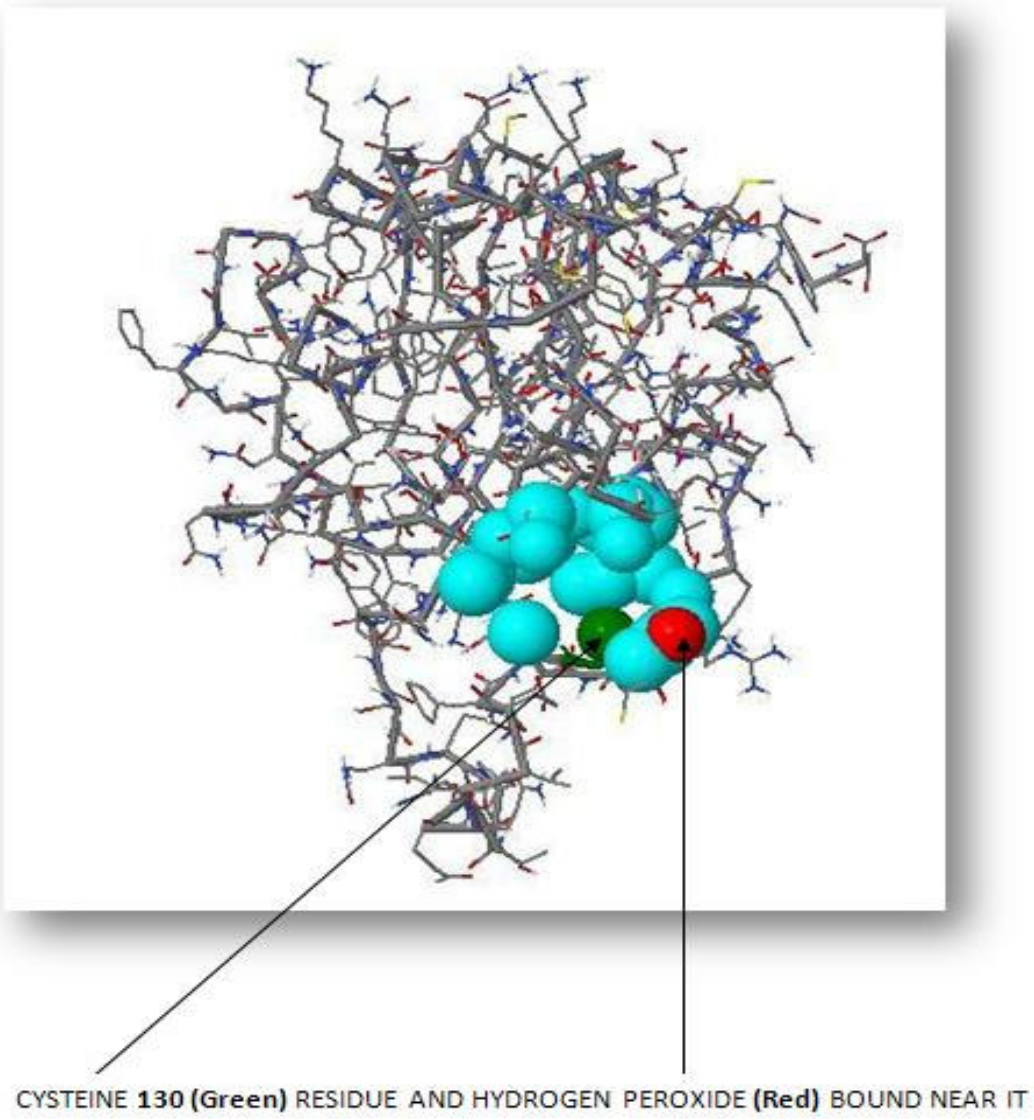

Fig. 5- Cysteine residue and hydrogen peroxide bound near it

Table 1- Summary of accessible surface area and rotamer calculations

RES. NUM.	RES. NAME	SCND STRUC	HBOND HBOND	BTURN BTURN	RES. ASA	FRAC. ASA	RES. VOL.	FRAC. VOL.	PHI PHI	PSI PSI	OMEGA OMEGA
33	ASN	CCC C			194.4	1.18	115.5	0.99	360.0	141.5	-167.8
34	GLY	CCC C			73.0	0.80	70.1	1.11	-177.1	144.0	-179.1
35	SER	CCC C			68.9	0.52	100.7	1.11	-175.8	-167.9	-173.1
36	CYS	CCC C			150.4	1.04	91.6	0.88	-92.6	-31.8	-167.5
37	GLY	CCC C			38.4	0.42	55.0	0.87	-106.6	167.2	175.5
38	MET	CCC C	40		148.4	0.68	148.1	0.91	-64.1	-67.8	-179.1
38	MET	CCH C	42,43	III	77.6	0.36	168.5	1.03	57.9	4.9	-172.8
40	GLY	HHH H	38,44	III	30.3	0.33	54.3	0.86	-73.4	-23.6	-177.5
41	ASN	HHH H	44	III	82.3	0.50	106.8	0.91	-76.6	-27.1	-179.2
42	ILE	HHH H	38,44	III	29.3	0.15	129.7	0.80	-70.2	-58.5	-179.8
43	SER	BHH H	38,40		42.3	0.32	118.3	1.31	-54.0	-1.5	177.0
44	GLN	BHH H	42,41		112.9	0.60	122.8	0.88	-105.5	-28.6	128.3
45	SER	BCC C	48		38.6	0.29	87.8	0.97	-28.5	-87.7	129.7
46	GLU	CCC C	49	I	26.7	0.14	129.1	0.97	21.6	-75.6	159.1
47	PRO	CCC C		I	93.5	0.60	98.8	0.86	-46.9	-35.0	-178.2
48	LYS	CCC C	44,45	I	165.9	0.77	153.3	0.99	-105.5	-12.6	-152.4
49	SER	CCC C	46	I	8.8	0.07	91.9	1.01	-171.7	-175.1	178.5
50	VAL	BCC C	182,53		0.0	0.00	139.6	1.03	-89.1	-11.6	-159.0
51	TYR	BCC C			2.3	0.01	193.7	1.01	-84.6	2.8	-171.9
52	ASP	BBB B	50		5.3	0.03	93.6	0.82	-117.9	21.7	-176.9
53	PHE	BBB B	50,65		17.5	0.08	184.9	0.94	-104.5	134.6	154.5
54	THR	BBB B			38.4	0.25	134.2	1.15	-103.6	130.2	-178.8
55	VAL	BBB B	63,63		12.2	0.07	149.1	1.10	-124.0	167.6	-170.0
56	LYS	BBB B	141		95.4	0.45	166.5	1.08	-105.1	139.9	171.2
57	ASP	CBC C	61,60	I	13.2	0.08	108.0	0.95	-90.8	-175.2	178.3
58	ALA	CCC C	139	I	67.2	0.54	99.2	1.14	-44.5	-29.0	-174.8
59	ARG	CCC C	57	I	190.5	0.78	150.3	0.86	-116.3	20.3	163.0
60	GLY	CCC C	57	I	43.7	0.48	51.4	0.82	73.0	32.3	176.9
61	ASN	BBC B	57		67.8	0.41	105.8	0.90	-110.0	142.1	-169.0
62	ASP	BBC B			45.6	0.29	119.0	1.05	-76.6	138.5	-175.7
63	VAL	BBC B	55,55		29.1	0.17	125.8	0.93	-135.1	107.2	172.4
64	ASP	BHC C	66,67		9.0	0.06	112.7	0.99	-74.1	123.7	-175.3
65	LEU	CHH H	53,68		0.0	0.00	159.4	0.98	-65.5	-7.7	-178.6
66	SER	CHH H	64,69	I	22.5	0.17	88.8	0.98	-82.0	-5.4	175.2
67	THR	CHH H	64,65	I	100.2	0.66	110.3	0.94	-72.6	-6.7	173.1
68	TYR	CCH C	65,71	I	30.5	0.13	193.5	1.01	-100.8	10.2	171.3
69	LYS	CCC C	66	I	123.0	0.57	160.5	1.04	-61.9	134.1	-180.0
70	GLY	CCC C	180		27.8	0.31	54.9	0.87	108.1	-6.1	-164.9

71	LYS	BBB B 68		49.8	0.23	159.1	1.03	-131.3	129.8	165.5
72	VAL	BBB B 105		0.0	0.00	123.3	0.91	-81.8	142.7	-166.8
73	LEU	BBB B 178		0.0	0.00	167.8	1.03	-130.7	152.1	-178.1
73	LEU	BBB B 107,105		0.0	0.00	161.3	0.99	-131.5	117.1	-164.5
75	ILE	BBB B 176,176		0.0	0.00	175.6	1.09	-114.4	115.1	-166.5
76	VAL	BBB B 109,107		2.0	0.01	145.6	1.07	-128.8	131.1	169.9
77	ASN	BBB B 173		0.0	0.00	134.9	1.15	-85.9	138.9	-171.8
78	VAL	BBB B 111,109		4.4	0.03	150.5	1.11	-128.2	156.1	-179.8
79	ALA	BCB B		34.2	0.28	147.6	1.69	-61.5	150.0	-176.9
80	SER	BCB B 130,111		5.4	0.04	119.8	1.32	-80.8	-19.0	-166.7
81	GLN	CCC C		35.5	0.19	186.6	1.34	-87.8	-178.8	-165.5
82	CYS	CCC C		90.8	0.63	106.1	1.01	-94.0	145.2	169.5
83	GLY	CCC C		29.9	0.33	78.7	1.25	132.5	122.0	-175.7
84	LEU	CCC C		71.0	0.34	160.0	0.98	-102.8	29.6	-166.5
85	THR	CCC C		130.0	0.86	96.2	0.82	-83.6	-27.8	177.4
86	ASN	CCC C 89	III	58.5	0.35	142.4	1.22	-57.2	149.4	-165.5
87	SER	CHC C 90	III	72.0	0.55	82.6	0.91	-70.7	-33.1	177.4
88	ASN	HHH H 91,92	III	16.1	0.10	167.4	1.43	-43.3	-35.8	-168.9
89	TYR	HHH H 86,93	III	18.1	0.07	260.7	1.36	-71.8	-39.3	-168.2
90	THR	HHH H 87,94		91.2	0.60	106.5	0.91	-73.9	-40.0	-174.1
91	GLU	HHH H 95,94		36.4	0.19	137.1	1.03	-76.5	-24.4	175.4
92	LEU	HHH H 88,96		9.7	0.05	185.0	1.13	-73.4	-41.1	171.3
93	THR	HHH H 89,97		45.5	0.30	123.1	1.05	-52.8	-39.2	-173.3
94	GLN	HHH H 90,98		68.0	0.36	123.0	0.88	-73.1	-43.5	174.7
95	LEU	HHH H 91,98		0.0	0.00	138.1	0.85	-47.5	-69.1	-167.6
96	TYR	HHH H 92,99	I	32.4	0.13	149.9	0.78	-49.8	-43.6	-158.1
97	GLN	HHH H 93,94	I	97.5	0.51	121.3	0.87	-76.2	-24.1	-179.0
98	LYS	HHH H 94,95	I	84.6	0.39	130.5	0.85	-81.5	-18.2	-124.5
99	TYR	CCC C 96	I	6.5	0.03	166.5	0.87	-157.8	36.7	146.5
100	LYS	BCC C 215		36.2	0.17	133.4	0.87	-112.9	-24.1	-174.7
101	ASP	BCC C 103		44.6	0.28	90.0	0.79	-76.9	-25.5	-150.4
102	GLN	BBC B 211		11.3	0.06	98.8	0.71	-118.1	29.1	-106.4
103	GLY	BBC B 101		2.3	0.03	44.7	0.71	-40.3	178.0	-176.8
104	LEU	BBB B		0.0	0.00	134.2	0.82	176.1	175.1	-178.3
105	GLU	BBB B 72,73		6.7	0.04	154.1	1.16	-160.7	148.4	174.1
106	ILE	BBB B		0.2	0.00	152.0	0.94	-117.6	132.4	-169.6
107	LEU	BBB B 73,76		0.0	0.00	166.0	1.02	-126.5	126.7	-172.6
108	ALA	BBB B 140,138		2.0	0.02	95.3	1.09	-124.0	120.1	-166.9
109	PHE	BBB B 76,78		0.8	0.00	214.0	1.09	-109.5	116.9	-171.2
110	PRO	BBB B 143,141		5.1	0.03	124.6	1.08	-77.6	166.6	-175.9

111	CYS	BBB B 78,80	0.1	0.00	122.7	1.17	-161.9	167.7	-170.6
112	ASN	BCC C	24.0	0.15	127.4	1.09	-147.4	56.3	-168.7
113	GLN	CCC C	62.2	0.33	158.2	1.14	-127.5	-8.6	-170.7
114	PHE	CCC C	31.2	0.14	185.2	0.95	-120.1	121.0	178.6
115	GLY	CCC C 117	32.4	0.36	58.4	0.93	49.4	48.8	177.9
116	SER	CCC C	34.0	0.26	98.1	1.08	-65.0	2.8	-171.1
117	GLN	CCC C 115	146.7	0.77	119.9	0.86	-106.5	29.6	-170.2
118	GLU	CCC C	102.0	0.54	129.1	0.97	-94.2	-55.8	-174.3
119	PRO	CCC C	37.8	0.24	105.2	0.91	-68.3	147.2	153.5
120	GLY	CCC C	91.1	1.00	49.0	0.78	-26.1	-39.4	-170.0
121	THR	CCC C	93.6	0.62	108.8	0.93	-133.8	74.4	179.3
122	ASN	CCC C 124	13.9	0.08	110.6	0.94	-97.6	-28.7	-170.7
123	GLU	CCC C	131.2	0.69	116.2	0.87	-50.8	-24.7	-171.9
124	GLN	CCC C 122	64.6	0.34	148.2	1.07	-59.7	132.3	-179.2
125	ILE	CCC C	156.0	0.79	134.0	0.83	-120.2	101.4	164.7
126	VAL	CCC C	119.1	0.69	114.0	0.84	-124.7	-7.1	-178.3
127	GLU	CCC C	56.2	0.30	130.8	0.98	-179.9	-55.8	177.1
128	PHE	CCC C	43.6	0.19	187.7	0.96	95.2	14.4	176.6
129	ALA	CCC C	12.6	0.10	94.1	1.08	-145.1	140.0	-168.8
130	CYS	CCC C 80,132	24.7	0.17	135.0	1.29	-67.2	145.0	-171.6
131	THR	CCC C	114.4	0.76	97.6	0.84	-80.1	1.9	-173.0
132	ARG	CBC C 130	151.2	0.62	164.9	0.94	-157.2	130.8	175.7
133	PHE	CBC C	31.0	0.14	212.0	1.08	-139.9	113.0	-157.9
134	LYS	CBC C	100.7	0.47	172.3	1.12	-96.7	117.8	-178.6
135	ALA	CBC C	49.3	0.40	96.7	1.11	-170.8	155.1	-170.0
136	GLU	CCC C	66.3	0.35	158.3	1.19	-81.9	-39.0	-171.8
137	TYR	BBB B	5.7	0.02	193.2	1.01	-81.9	145.5	-169.1
138	PRO	BBB B 108	55.5	0.36	137.3	1.19	-69.5	135.3	173.9
139	ILE	BBB B 58	16.3	0.08	165.8	1.03	-107.1	138.2	-165.9
140	PHE	BBB B 108	4.1	0.02	173.7	0.89	-107.5	-170.4	176.9
141	ASP	BBB B 56,110	53.0	0.34	126.9	1.12	-77.0	171.9	-167.5
142	LYS	BBB B	86.4	0.40	160.6	1.04	-83.0	151.3	-175.7
143	VAL	CBB B 110	24.7	0.14	146.3	1.08	-152.9	152.5	169.2
144	ASP	CCB C 150	40.1	0.25	123.9	1.09	-85.6	140.8	-179.5
145	VAL	CCC C	0.0	0.00	135.6	1.00	-105.6	-15.4	-168.1
146	ASN	CCC C	40.8	0.25	129.6	1.11	-140.1	152.3	173.7
147	GLY	CCC C 148,150	65.2	0.72	56.7	0.90	90.6	-157.7	-158.6
148	ASN	CCC C	144.1	0.87	101.9	0.87	-87.0	-4.9	-172.4
148	ASN	CCC C 147	102.0	0.62	102.0	0.87	-130.2	18.8	177.4
150	ALA	CCC C 147	26.4	0.21	82.0	0.94	-60.8	130.8	-175.2
150	ALA	CHC C 144,154	14.2	0.11	97.6	1.12	-55.7	145.8	-173.4

152	PRO	HHH H 155,156		70.9	0.46	112.9	0.98	-62.2	-16.8	175.9
153	LEU	HHH H 157,156		1.5	0.01	175.8	1.08	-62.1	-41.3	-175.1
154	TYR	HHH H 150,158		0.9	0.00	233.6	1.22	-75.8	-19.1	-179.6
155	LYS	HHH H 152,158		152.5	0.71	156.5	1.02	-72.3	-46.7	-178.8
156	PHE	HHH H 152,159		31.9	0.14	175.5	0.90	-59.9	-46.8	-179.3
157	LEU	HHH H 153,159		0.0	0.00	160.0	0.98	-62.8	-27.4	-176.7
158	LYS	HHH H 154,155		40.9	0.19	166.9	1.08	-80.8	-4.7	-179.5
159	SER	HHH H 156,162		65.2	0.50	78.9	0.87	-89.4	-21.4	-177.8
159	SER	CCC C 157,162	III'	10.5	0.08	107.2	1.18	-43.1	138.1	165.7
161	LYS	CCC C	III'	129.5	0.60	161.8	1.05	65.5	38.2	166.0
162	GLY	CCC C	III'	78.4	0.86	52.8	0.84	68.2	40.5	179.1
162	GLY	CCC C 159,159	III'	29.6	0.33	62.8	1.00	52.5	138.2	-178.8
164	ILE	CCC C 166		108.7	0.55	145.2	0.90	-116.5	-2.8	-179.9
165	PHE	CCC C		212.9	0.94	154.5	0.79	62.3	17.8	179.8
166	GLY	CCC C 164		52.8	0.58	54.3	0.86	-159.2	26.0	-175.1
167	ASP	CCC C		18.6	0.12	145.2	1.28	-91.6	49.2	-169.0
168	ASN	CCC C		90.2	0.55	152.1	1.30	-106.0	150.2	-175.9
169	ILE	CCC C		7.1	0.04	134.5	0.83	-90.7	122.8	169.3
170	LYS	CCC C		162.0	0.76	147.1	0.95	-100.3	-5.0	176.4
171	TRP	CCC C		105.5	0.40	194.2	0.84	-158.2	169.5	162.4
172	ASN	CCC C		15.3	0.09	134.5	1.15	-45.3	153.6	162.2
173	PHE	CCC C 77		50.0	0.22	186.9	0.96	75.9	49.1	178.0
174	SER	BBB B		6.6	0.05	114.6	1.26	-105.4	76.8	-174.3
175	LYS	BBB B 188		7.1	0.03	202.3	1.31	-64.0	151.0	-177.0
176	PHE	BBB B 75,75		1.1	0.00	203.0	1.04	-119.3	123.9	179.9
177	LEU	BBB B 184,186		4.6	0.02	154.0	0.94	-98.2	131.3	-178.7
178	VAL	BCB B 73		0.0	0.00	131.8	0.97	-105.5	-165.0	177.8
179	ASP	BCB B 183,182	I	21.8	0.14	122.5	1.08	-137.4	176.9	176.6
180	LYS	CCC C 70	I	78.9	0.37	147.3	0.96	-61.7	-25.0	-168.2
181	ASP	CCC C 179	I	82.2	0.52	117.7	1.03	-99.2	-12.8	171.4
182	GLY	CCC C 179,50	I	0.0	0.00	66.5	1.06	102.6	15.6	-176.5
183	ASN	CCC C 179		62.7	0.38	117.6	1.00	-108.2	151.2	-172.1
184	VAL	CCC C		7.0	0.04	143.9	1.06	-91.0	139.6	-167.3
184	VAL	BCB B 177		50.1	0.29	115.4	0.85	-121.6	-25.4	-179.9
186	ASP	BBB B 177		30.5	0.19	115.8	1.02	-158.9	178.5	-171.9
187	ARG	BBB B		44.3	0.18	174.9	1.00	-163.9	147.1	-168.5
188	TYR	CBB B 175		57.9	0.24	205.7	1.08	-144.8	147.7	-169.0
189	ALA	CCC C 191	I	59.5	0.48	88.5	1.01	-77.0	166.2	-178.3
190	PRO	CCC C 191	I	26.7	0.17	123.0	1.07	-59.1	-30.0	-156.2
191	THR	CCC C	I	113.2	0.75	100.1	0.86	-81.6	-7.3	-179.8

191	THR	CCC	C	189,190	I	46.3	0.31	118.8	1.02	-85.0	120.4	-168.0
193	VAL	CHC	C	195,196		50.1	0.29	115.6	0.85	-75.7	153.5	-174.3
194	PRO	CHH	H	196,197		1.0	0.01	124.7	1.08	-67.8	-20.7	-168.8
195	SER	CHH	H	198,197		35.8	0.27	91.7	1.01	-71.4	-15.2	-176.9
196	GLN	CHH	H	193,194		127.9	0.68	121.2	0.87	-86.9	3.7	179.9
197	HIS	CCH	C	194,201		2.4	0.01	163.1	1.05	-113.7	16.4	-171.5
198	ARG	HHH	H	202,201		42.7	0.18	181.4	1.03	-70.3	-52.3	-179.1
199	GLU	HHH	H	202,202		123.2	0.65	123.4	0.93	-43.9	-56.2	-178.6
200	GLY	HHH	H	204,202		15.3	0.17	74.4	1.18	-69.1	-27.8	177.9
201	CYS	HHH	H	197,198		0.0	0.00	113.4	1.09	-64.7	-27.9	-152.6
202	GLU	HHH	H	198,199		52.7	0.28	110.2	0.83	-85.7	-39.8	-163.1
202	GLU	HHH	H	199,200		123.7	0.65	119.1	0.89	-82.1	-19.3	-177.2
204	THR	HCH	H	200,207	I	28.3	0.19	112.1	0.96	-77.8	-174.3	-176.5
205	ALA	CCC	C	207	I	47.1	0.38	81.2	0.93	-62.7	-2.8	-173.2
206	GLY	CCC	C	204,209	I	0.0	0.00	52.6	0.83	-84.9	-5.9	165.8
207	ASP	CCH	C	204,209	I	77.6	0.49	93.8	0.82	64.0	21.6	157.1
208	CYS	CCH	C	202,206		52.0	0.36	90.2	0.86	89.3	2.6	-148.2
209	MET	CCH	C	206,207		116.8	0.53	135.2	0.83	-143.1	-3.2	120.9
210	SER	CCC	C			7.0	0.05	75.4	0.83	143.1	-23.7	-127.9
211	ALA	CCC	C	102		0.0	0.00	52.6	0.60	120.4	-59.0	-140.6
212	GLN	CCC	C			63.7	0.34	110.9	0.80	-71.5	-39.2	148.5
213	GLY	CCC	C	216		26.3	0.29	56.0	0.89	-30.0	-73.8	107.9
214	ARG	CCC	C			79.5	0.33	168.8	0.96	14.6	-51.3	172.3
215	PRO	CCC	C	100		68.8	0.44	95.4	0.83	-80.3	-18.1	-166.0
216	ASN	CCC	C	213		132.0	0.80	98.1	0.84	-82.0	360.0	360.0

Table 2- Summary of hydrogen bond calculations

HBOND ACCPT(CO)	HBOND DONOR(NH)	HBOND DIST.	HBOND ANGLE
VAL 76	PHE 109	2.08	169.33
ASN 77	PHE 173	1.98	152.54
VAL 78	GLY 40	2.33	141.46
MET 38	GLY 40	2.42	122.09
SER 80	CYS 130	1.70	165.39
MET 38	ILE 42	2.27	141.95
ASN 86	TYR 89	2.37	130.57
MET 38	SER 43	1.96	143.03
SER 87	THR 90	2.29	144.09
GLY 40	GLN 44	2.81	152.96
ASN 88	GLU 91	2.94	149.70
ASN 41	GLN 44	2.07	119.90
ASN 88	LEU 92	2.10	164.58
ILE 42	GLN 44	2.42	115.51
TYR 89	THR 93	1.90	161.70
SER 45	LYS 48	1.73	154.96
THR 90	GLN 94	2.04	165.10
GLU 46	SER 49	2.63	125.94
GLU 91	LEU 95	1.89	149.56
VAL 50	PHE 53	2.57	115.43
GLU 91	GLN 94	2.59	135.97
PHE 53	LEU 63	1.95	169.46
LEU 92	TYR 96	1.70	143.73
VAL 55	VAL 63	1.93	167.54
THR 93	GLN 97	1.86	159.73
LYS 56	ASP 141	2.13	118.84
GLN 94	LYS 98	2.11	149.62
ASP 57	GLY 60	1.83	124.59
LEU 95	LYS 98	1.95	138.89
ASN 61	ASP 57	2.23	158.04
TYR 96	TYR 99	1.88	121.26
VAL 63	VAL 55	2.08	124.44
LYS 100	PRO 215	2.90	141.67
ASP 64	SER 66	2.70	124.66
ASP 101	THR 67	2.17	137.34
GLU 105	GLY 103	2.20	105.41
LEU 65	TYR 68	2.12	129.98
LEU 107	LEU 73	2.40	162.86
SER 66	LYS 69	1.94	111.07
ALA 108	VAL 76	2.19	171.52
TYR 68	LYS 71	2.15	126.90
PHE 109	PHE 140	2.05	162.59
VAL 72	GLU 105	2.54	155.40
PRO 110	VAL 78	2.43	143.31
LEU 73	VAL 143	1.97	149.95
CYS 111	LEU 107	2.26	149.88
LEU 73	SER 80	2.03	174.71
GLY 115	GLN 117	2.67	110.38
		2.45	119.65

ASN 122	GLN 124	2.75	130.96
CYS 130	ARG 132	2.83	119.34
PRO 138	ALA 108	2.03	167.37
ILE 139	ALA 58	2.59	110.43
ASP 141	PRO 110	3.15	133.01
ASP 144	ALA 150	2.20	134.78
GLY 147	ASN 148	2.94	119.43
GLY 147	ALA 150	2.47	103.54
ALA 150	TYR 154	2.32	143.32
PRO 152	LYS 155	2.50	136.99
PRO 152	PHE 156	2.22	153.12
LEU 153	LEU 157	1.93	161.94
LEU 153	PHE 156	2.70	142.49
TYR 154	LYS 158	2.34	151.68
LYS 155	LYS 158	2.37	143.10
PHE 156	SER 159	1.96	131.08
LEU 157	SER 159	2.36	127.86
SER 159	GLY 162	2.17	136.63
SER 159	GLY 162	2.61	135.51
ILE 164	GLY 166	2.92	132.33
LYS 175	TYR 188	2.95	149.28
PHE 176	ILE 75	1.77	159.36
LEU 177	VAL 184	2.37	155.78
ASP 179	GLY 182	2.49	129.83
LYS 180	GLY 70	2.38	134.31
GLY 182	VAL 50	1.95	174.05
ASN 183	ASP 179	3.02	143.31

ASP 186	LEU 177	2.75	145.10
ALA 189	THR 191	2.36	129.53
PRO 190	THR 191	2.74	128.61
VAL 193	SER 195	3.07	139.90
VAL 193	GLN 196	2.33	137.65
PRO 194	GLN 196	3.00	134.82
PRO 194	HIS 197	1.96	122.03
SER 195	ARG 198	2.46	103.38
SER 195	HIS 197	2.88	114.64
HIS 197	CYS 201	2.07	168.66
ARG 198	GLU 202	2.14	163.52
ARG 198	CYS 201	2.30	160.73
GLU 199	GLU 202	2.24	147.01
GLU 199	GLU 202	2.13	166.11
GLY 200	THR 204	2.32	153.20
GLY 200	GLU 202	2.52	141.07
THR 204	ASP 207	2.04	130.82
ALA 205	ASP 207	2.93	119.29
GLY 206	MET 209	2.43	130.60
ASP 207	MET 209	2.85	126.99
ALA 211	GLN 102	1.47	122.75
GLY 213	ASN 216	2.80	160.72

